Effect of Al_2O_3 passivation layer in irradiated n-on-p strip sensors

27th RD50 Workshop, 2-4 Dec. 2015

T. Peltola[1], J. Härkönen[1]

[1]Helsinki Institute of Physics, P.O. Box 64, FI-00014 University of Helsinki, Finland

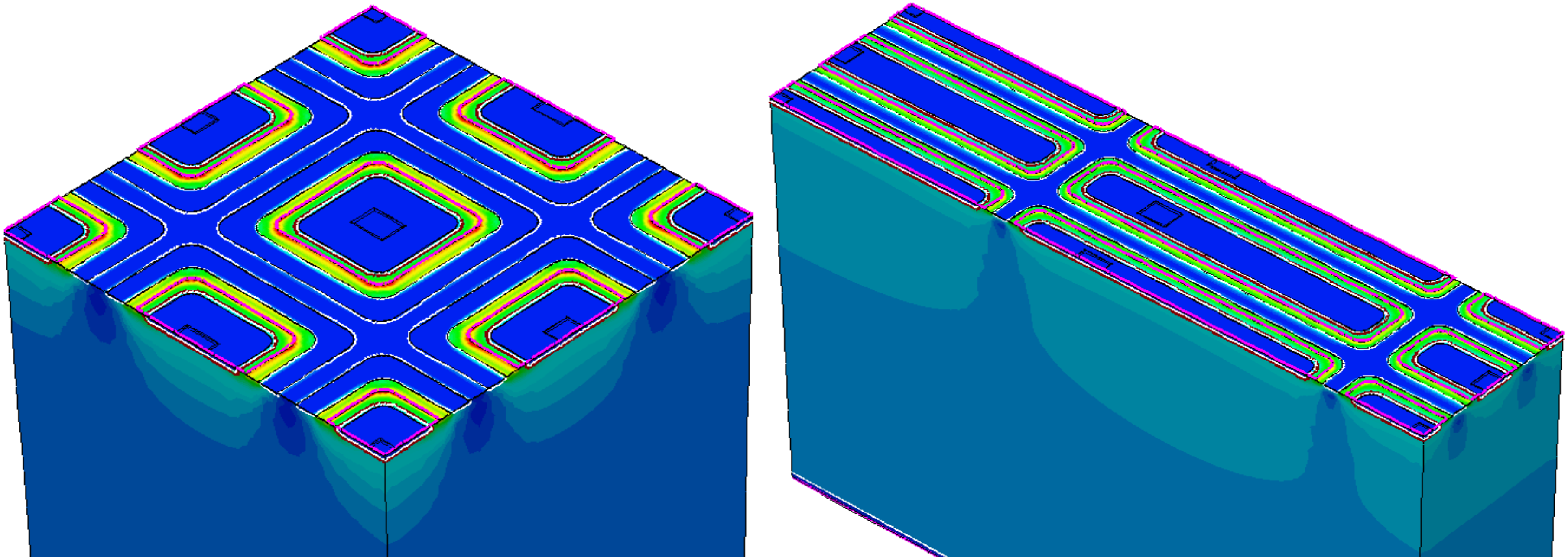

Outline

- ☐ **Motivation**
- ☐ **Non-irradiated strip sensors:**
  - Simulated alumina vs p-stop/p-spray
    - R_{int}, C_{int} & V_{bd}
- ☐ **Accumulation of negative oxide charge:**
  - MOS structure measurements & simulations
- ☐ **Al_2O_3 layer vs p-stop/p-spray in strip sensors:**
  - Proton irradiated Φ=2e15 $n_{eq}cm^{-2}$:
    - CV/IV & C_{int}
    - CCE & CCE loss between strips
- ☐ **Summary & Conclusions**

Motivation

Segmented n-on-p sensors: Challenges

- ❑ **Positive oxide charge → need for isolation implantations → requires more:**
  - Mask levels (=price)
  - High temperature processing steps
- ❑ Finer granularity increases local electric fields → lower breakdown voltage
- ❑ More implants mean higher capacitances (=noise, lower rise time of signal)

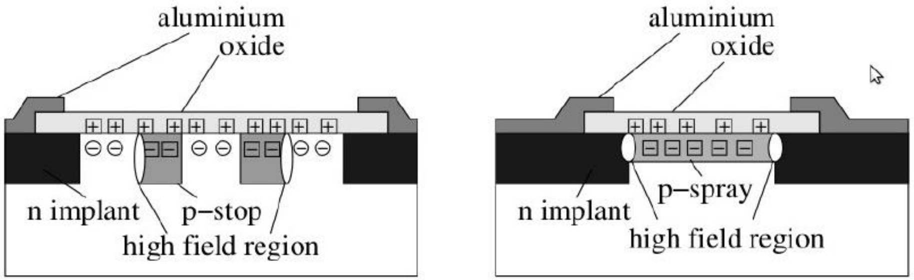

(a) *p*-Stops

(b) *p*-Spray

Figure by Tilman Rohe

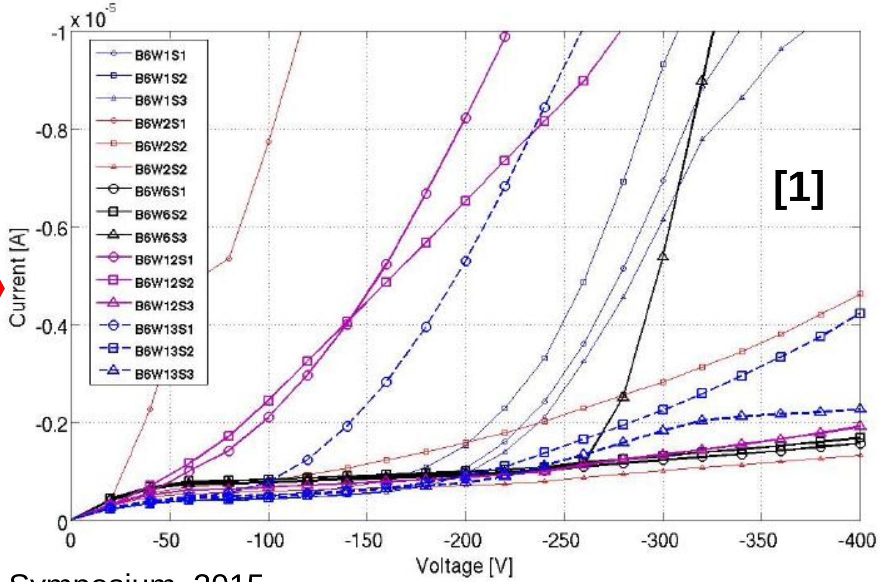

[1]

[1] J. Härkönen et al., 10th Hiroshima Symposium, 2015

ALD for radiation hard detectors

Atomic Layer Deposition (ALD)

- provides many potentially interesting material systems, e.g. high ε materials HfO_2, ZrO_2 etc.
- With ALD one can tailor amount and **type of oxide charge**
- ALD is pinhole free deposition → practically stress free
- ALD is applicable on large surfaces
- ALD is low temperature process, typically ~300° C

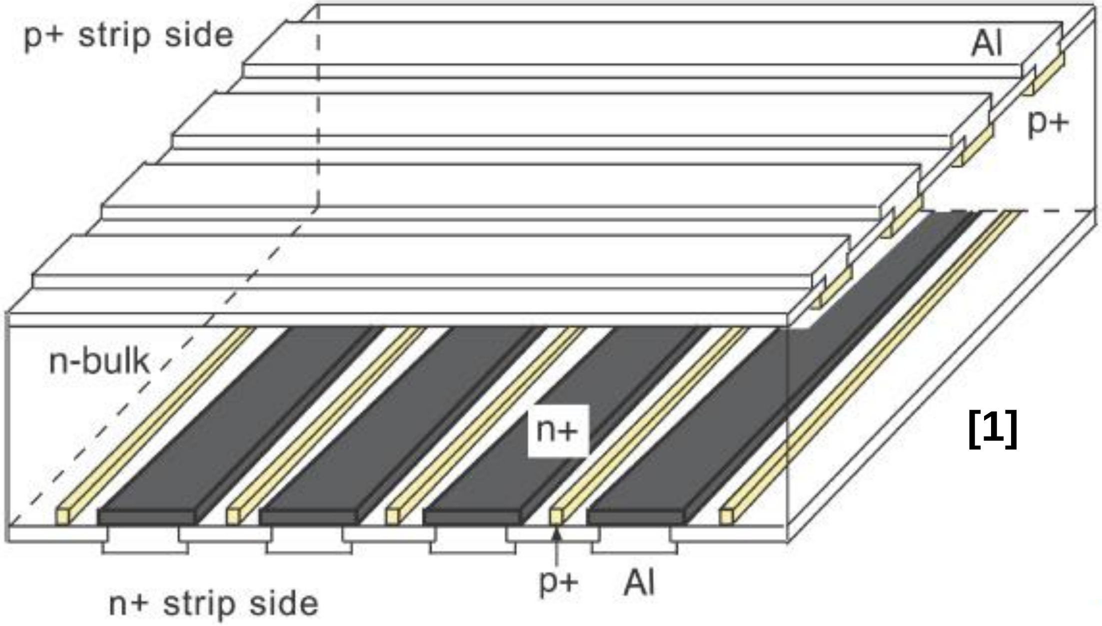

[1]

ALD grown Al_2O_3: Electrical passivation

- Studied by µPCD method
- Thermally dry oxidized wafer with very high bulk lifetime
- Assumption: SiO_2 passivation reduces $S_r \rightarrow 0$
- ALD deposition of Al_2O_3
- Subsequent annealing at 370^0C / 30min

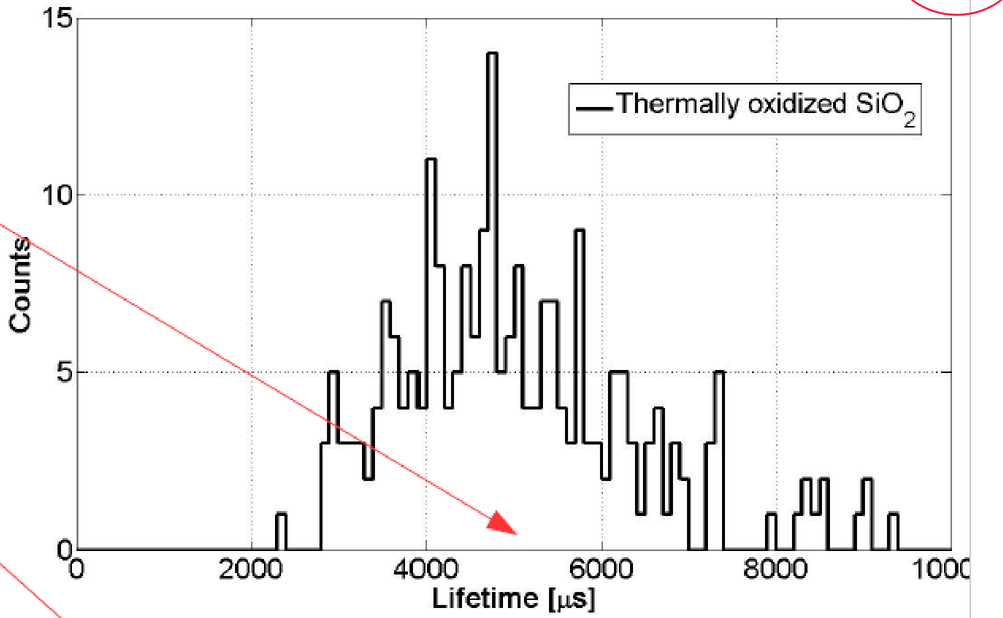

52 nm Al_2O_3:

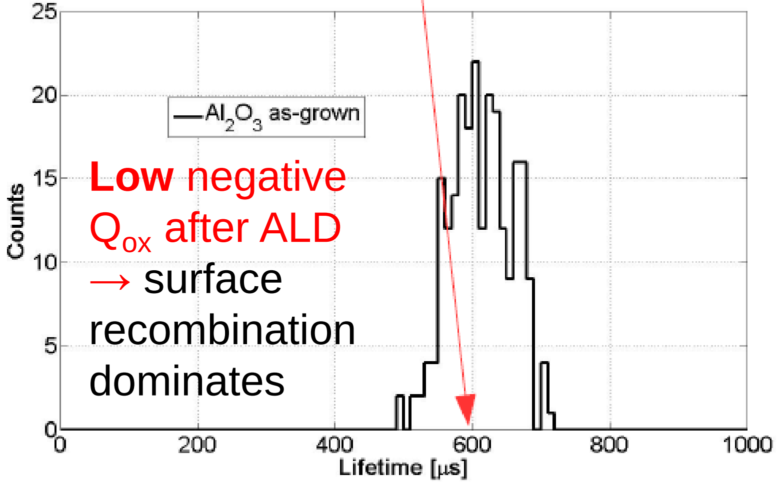

Low negative Q_{ox} after ALD → surface recombination dominates

[1]

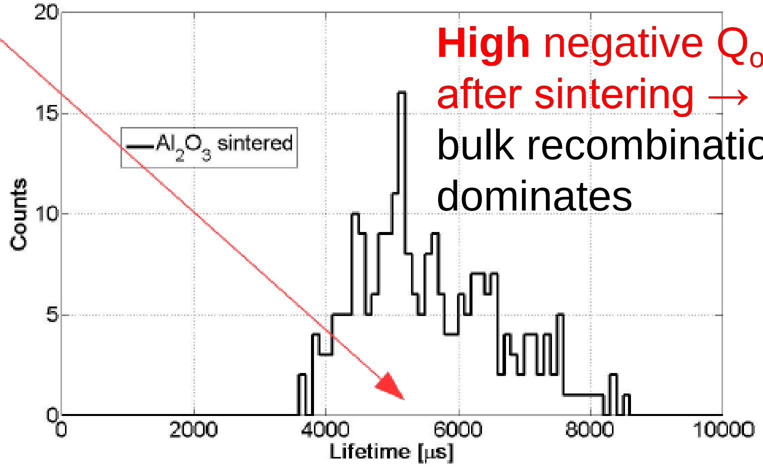

High negative Q_{ox} after sintering → bulk recombination dominates

Non-irradiated strip sensors

Simulation structures & parameters

- 200 µm thick n-on-p (V_{fd}=30 V) 3-strip structure @ T=293 K
- Pitch=55 µm, implant width=30 µm, MO=3 µm, DC-coupled

- **Double p-stop:** width=2 µm, depth=1.5 µm, spacing=4 µm, N_p = 5e16 cm^{-3}
- **p-spray:** depth=1.0 µm, N_p=1e16 cm^{-3}
- **No isolation structures:** SiO_2 & Al_2O_3 (alumina) passivation layers with opposite sign interface charge densities Q_f

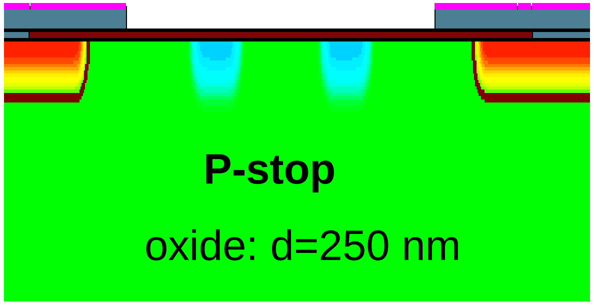

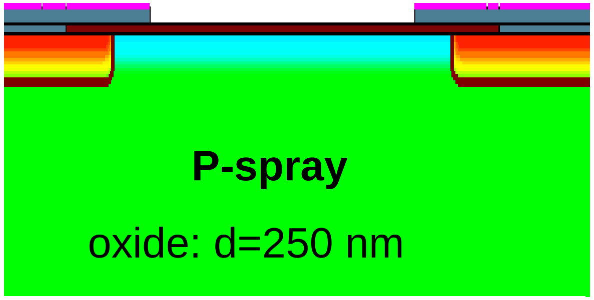

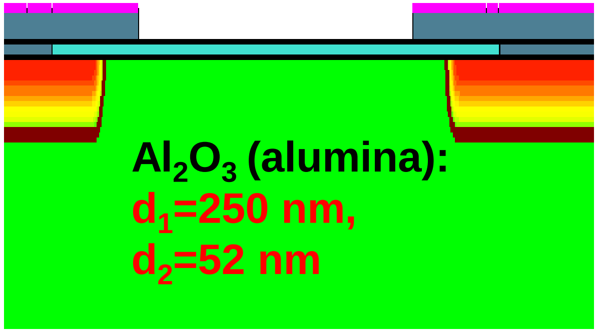

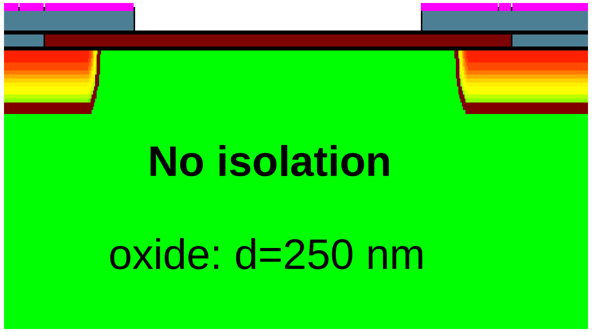

Q_f=(0.5-1)e11 cm^{-2}: R_{int} & C_{int}

Simulated R_{int} & C_{int} for typical values of Q_f in non-irradiated sensor:

- ❑ **non-isolated:** strips shorted
- ❑ **p-spray:** strips isolated, highest C_{int} values
- ❑ **p-stop:** strips isolated, low C_{int}
- ❑ **250 nm alumina:** strips isolated, increased Q_f → more holes at the accumulation layer → higher C_{int}
- ❑ **52 nm alumina:** 4 orders lower R_{int}, higher voltage needed for geom. C_{int}

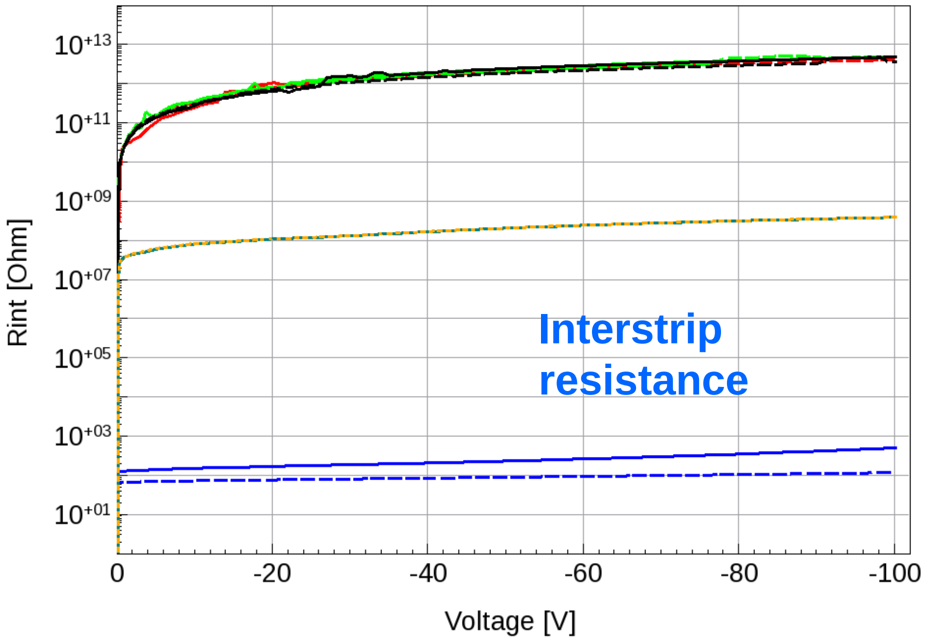

Interstrip resistance

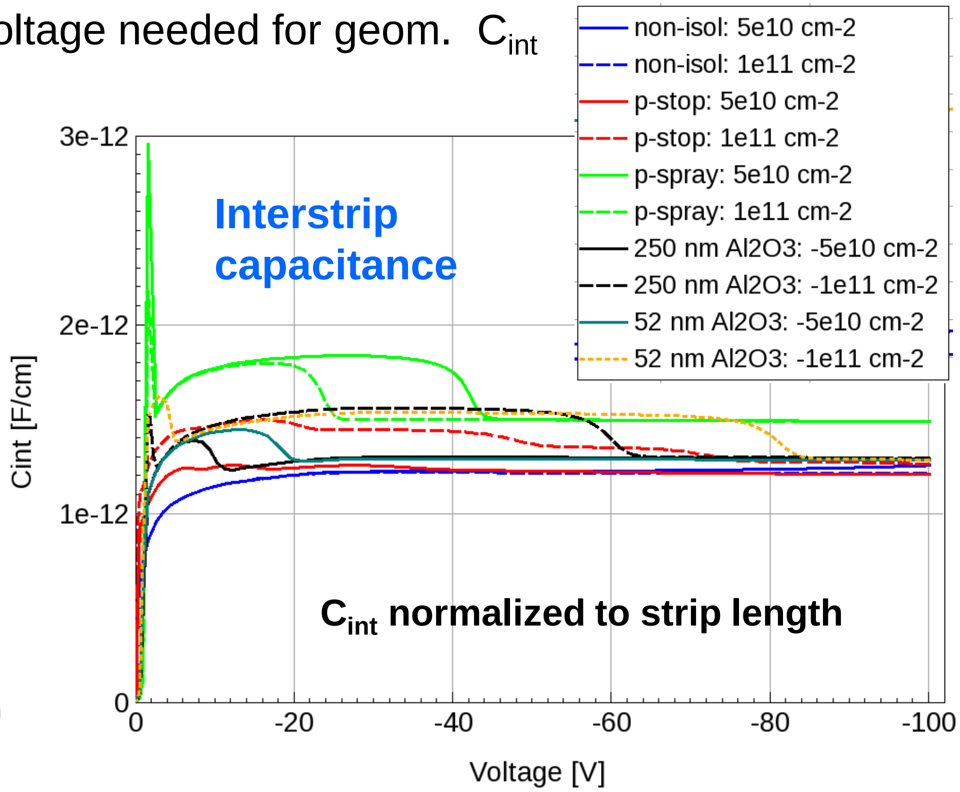

Interstrip capacitance

C_{int} normalized to strip length

Q_f=5e11 cm^{-2}: R_{int} & C_{int}

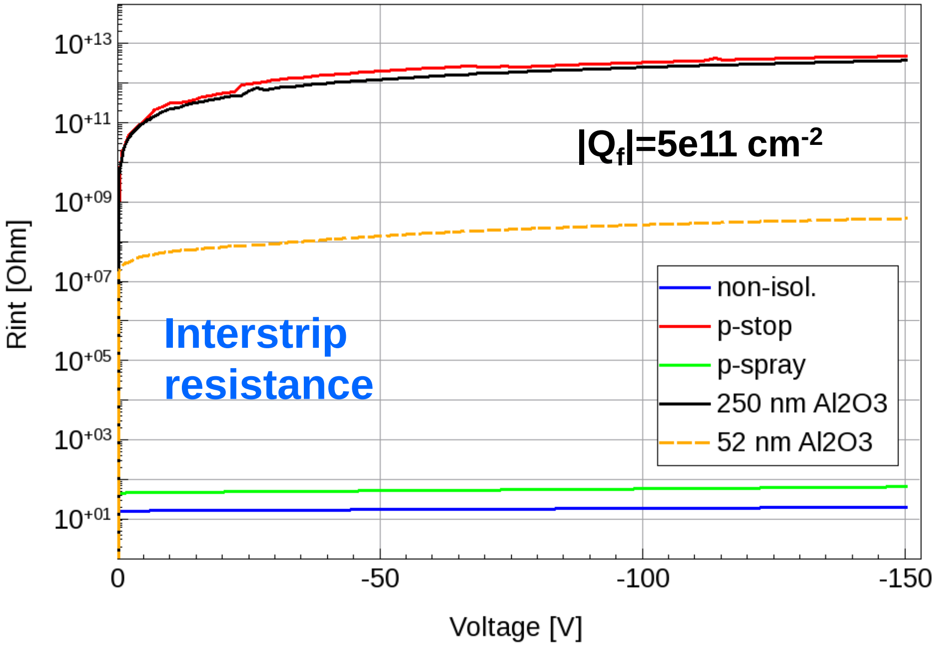

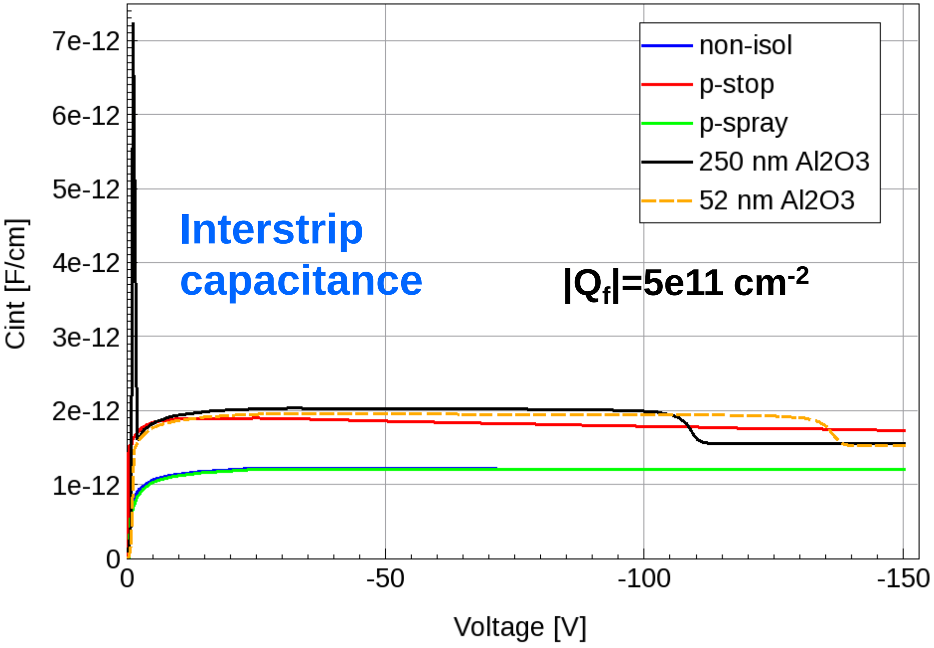

- ☐ **non-isolated & p-spray:** strips shorted
- ☐ **p-stop:** strips isolated
- ☐ **250 nm alumina:** strips isolated, highest C_{int} @ V < 110 V
- ☐ **52 nm alumina:** 4 orders lower R_{int}, higher voltage needed for low C_{int}, no initial peak in C_{int}

Thicker alumina layer → higher R_{int}, lower C_{int}

P-stop vs thick alumina: essentially equal surface properties

Breakdown voltage: p-stop vs alumina

- ☐ **p-stop:** higher Q_f → more acceptor levels at p-stops are compensated by electrons → lower E-fields & higher V_{bd} (also lower R_{int})
- ☐ **250 nm alumina:** higher Q_f → more holes at accumulation layer → higher E-fields & lower V_{bd}; $|V_{bd}|$ > 1 kV @ highest Q_f values for non-irradiated sensor
- ☐ **52 nm alumina:** thinner layer results in ~300 V lower V_{bd} for each Q_f

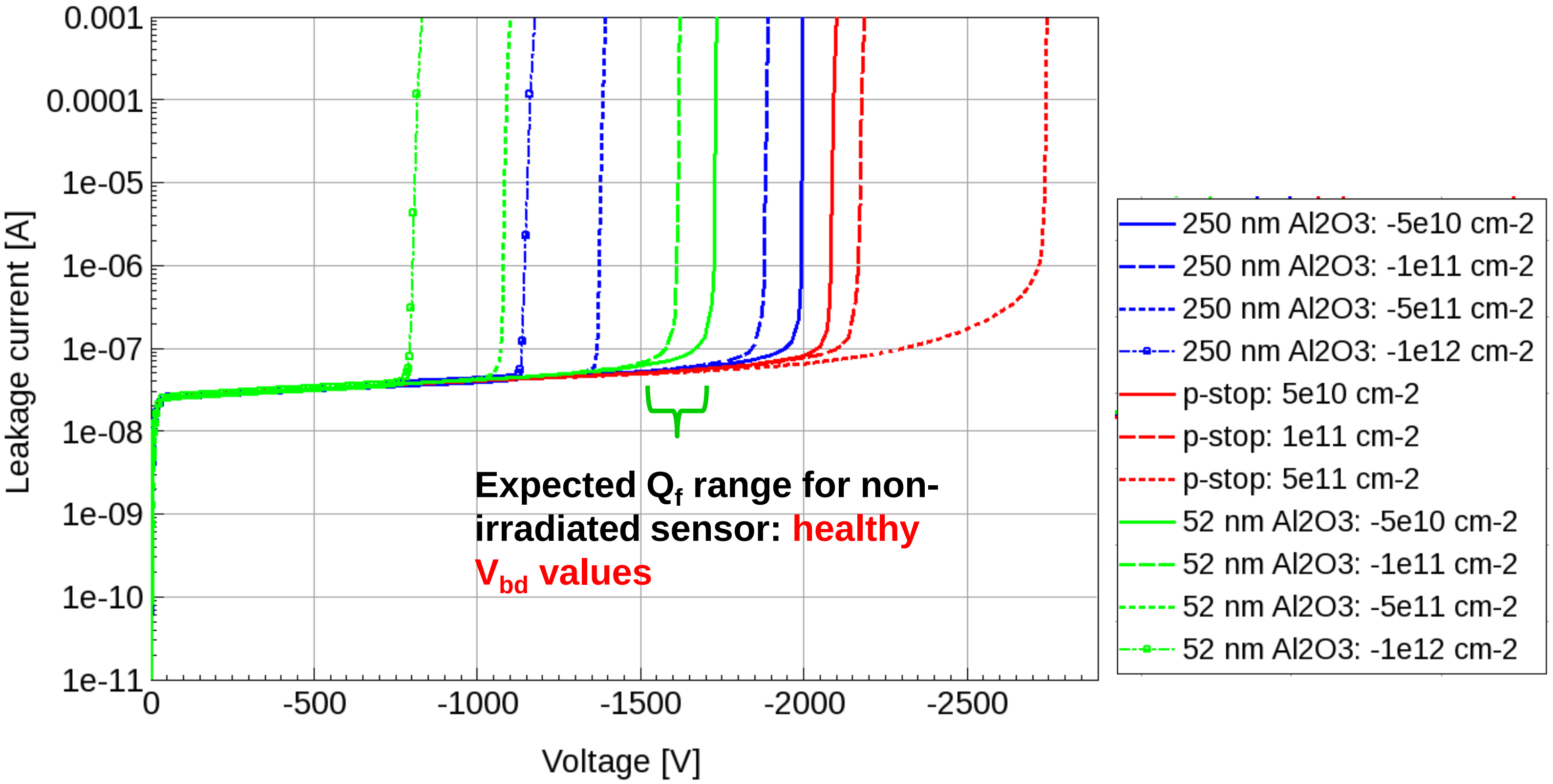

Expected Q_f range for non-irradiated sensor: healthy V_{bd} values

Irradiated MOS & strip sensors

MOS-structure: Measured & simulated V_{fb}

- γ-irradiated MOS test structure with 40 nm thick Al_2O_3 layer
- Shift of V_{fb} to higher forward bias voltage → accumulation of negative oxide charge
- Simulations of identical structure verify the observed behavior

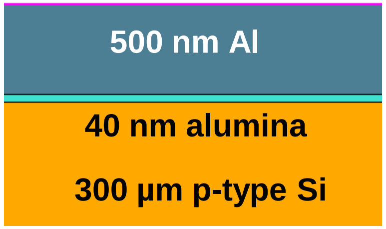

500 nm Al

40 nm alumina

300 µm p-type Si

[1]

Co60 gamma irradiated Al_2O_3 capacitor.

Flat band voltage shift ***towards to right*** indicates accumulation of negative oxide charge

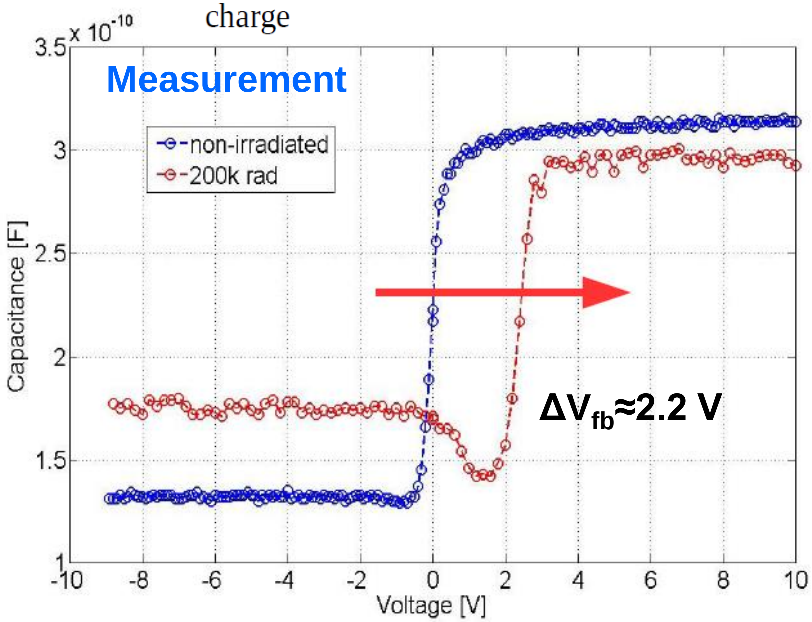

- **Modelled γ-irradiation induced surface damage:** increased Q_f
- **Q_f with N_{it}:** No effect to V_{fb}, affects only C offset

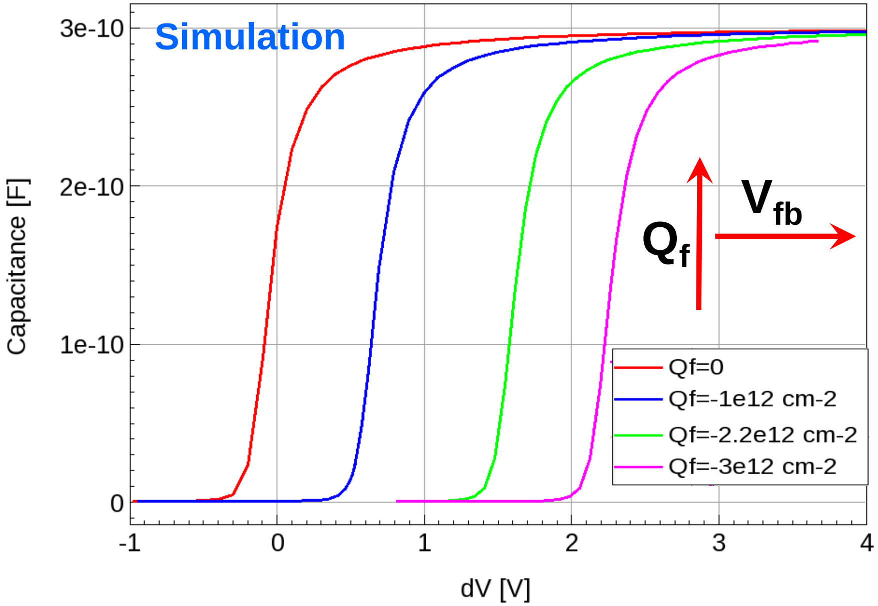

MOS-structure: Extraction of Q_f

- **Simulation as an extension of measurement:** find interface charge density Q_f corresponding to measured ΔV_{fb}
- Linear increase of ΔV_{fb} with Q_f → use slope & measured ΔV_{fb}

Simulation: C^{-2} vs ΔV

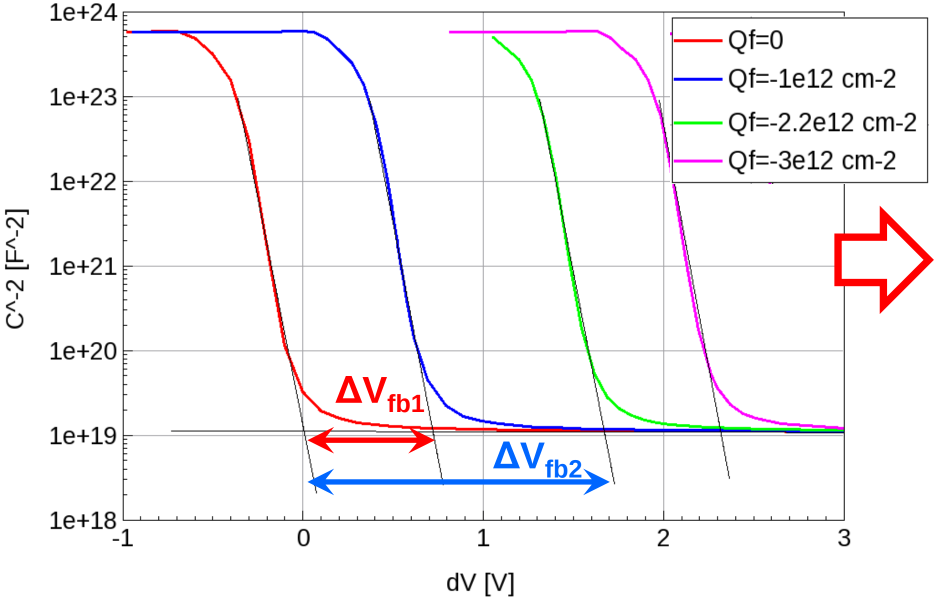

Q_f vs ΔV_{fb}

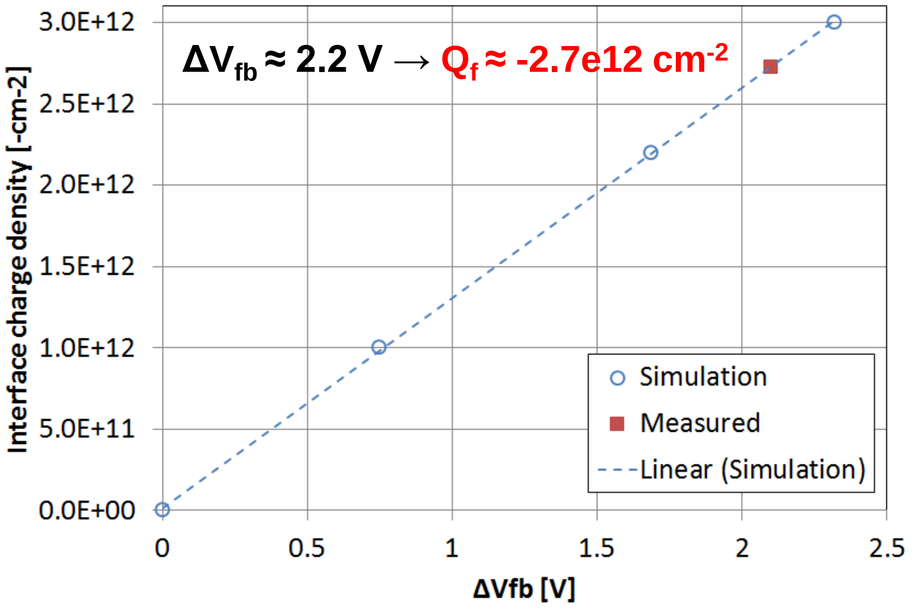
$\Delta V_{fb} \approx 2.2$ V → $Q_f \approx -2.7e12$ cm^{-2}

- **Resulting estimation of Q_f:** significant accumulation of negative oxide charge density at Al_2O_3/Si interface

Strips @ Φ=2e15 $n_{eq}cm^{-2}$: LC

- ☐ 3.88 cm*3.78 cm*298 µm n-on-p 3-strip structure, **Al_2O_3:** thickness=52 nm
- ☐ Pitch=80 µm, implant width=10 µm, MO=2 µm, AC-coupled

} **As in measured sensor**

- ☐ **Defects:** non-uniform 3-level model, Φ=2e15 $n_{eq}cm^{-2}$ → V_{fd}≈0.8-1 kV (model validated only up to ~1.5e15 $n_{eq}cm^{-2}$)
- ☐ Simulated & calculated LC normalized to T=-53.4° C by α(219.6 K) = 1.35e-20 A/cm
- ☐ **Q_f = 1.8e12 cm^{-2}: alumina:** Simulation converges only when interface donor traps added (E_V+0.6 eV)

- ☐ **Alumina: CM affects the simulated LC** (-4e10 cm^{-2} max value for simulation @ 1.1 kV without N_{it})

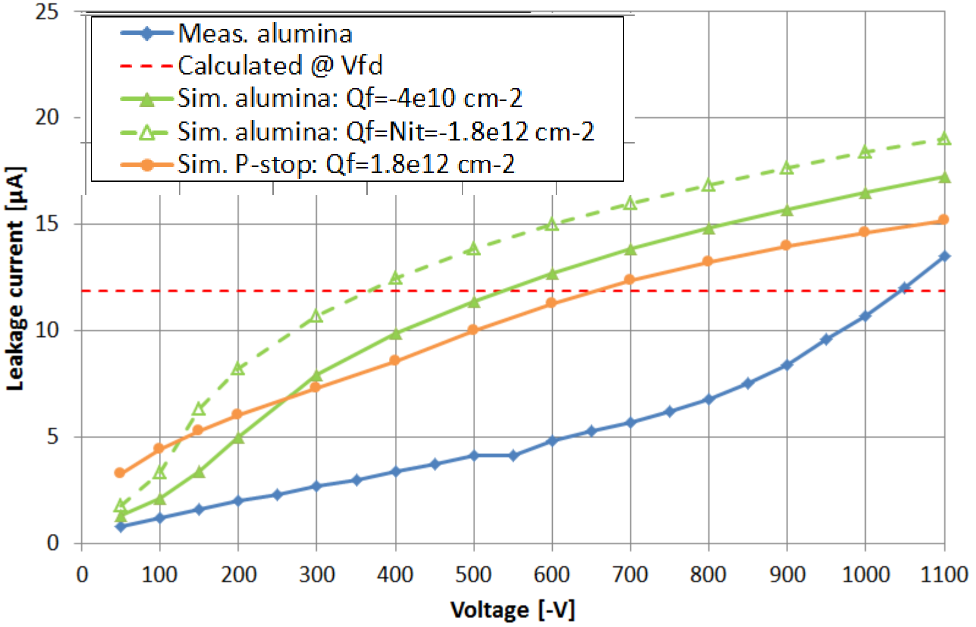

Alumina: LC ratio of measured to simulated

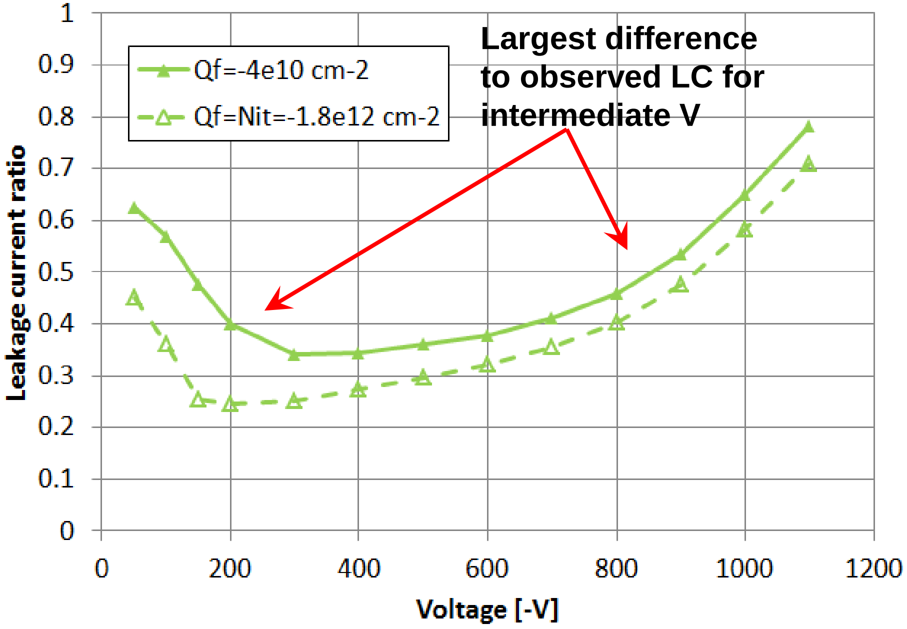

Largest difference to observed LC for intermediate V

Strips @ Φ=2e15 $n_{eq}cm^{-2}$: Simulated CV & C_{int}

❑ Corresponding CV to LC simulations on previous slide @ T=253 K

❑ P-stop CV-curve normalized to alumina curve due to higher Q_f value → higher charge in sensor

❑ **Q_f = 1.8e12 cm^{-2}:** Alumina C_{int} stays below p-stop values also at reduced N_{it} (no convergence below N_{it} = 1.2e12 cm^{-2} due to high E-fields)

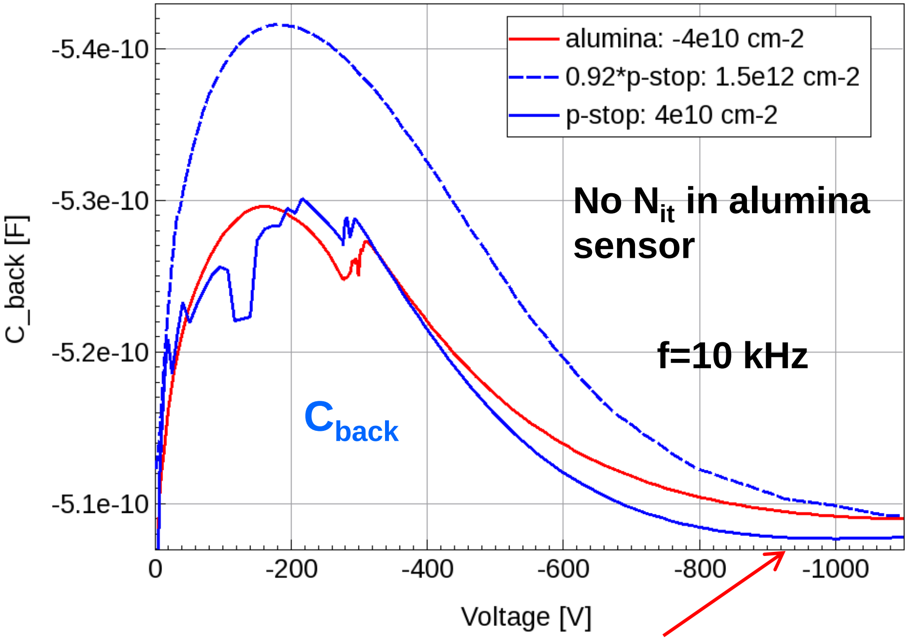

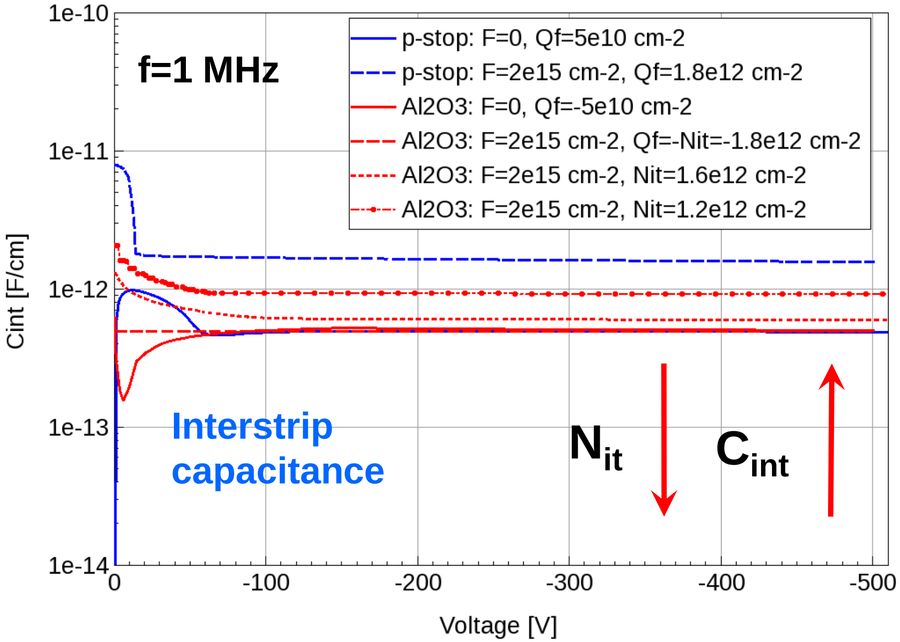

Lower C_{back} for p-stop @ equal $|Q_f|$
→ accumulation layer electrons
compensated by acceptors

❑ **Irradiated alumina sensor with N_{it}:**
Very low noise contribution from C_{int}

Strips @ Φ=2e15 $n_{eq}cm^{-2}$: Measured CCE

- ☐ ~300 µm thick n-on-p MCz-Si strip detector with ALD-grown Al_2O_3 insulator
- ☐ Full charge recorded from the telescope's non-irradiated reference planes ~40 ADC

SNR vs Voltage

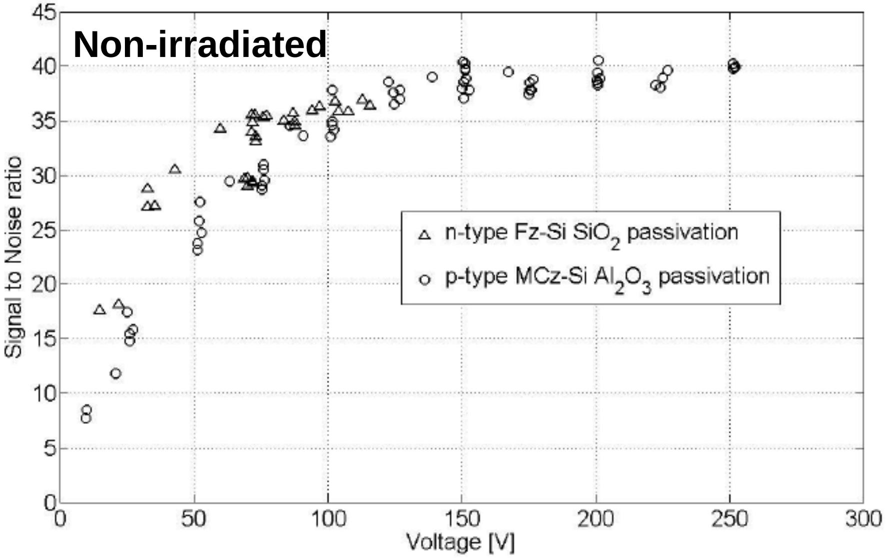

[1]

CC vs Voltage @ T=253 K

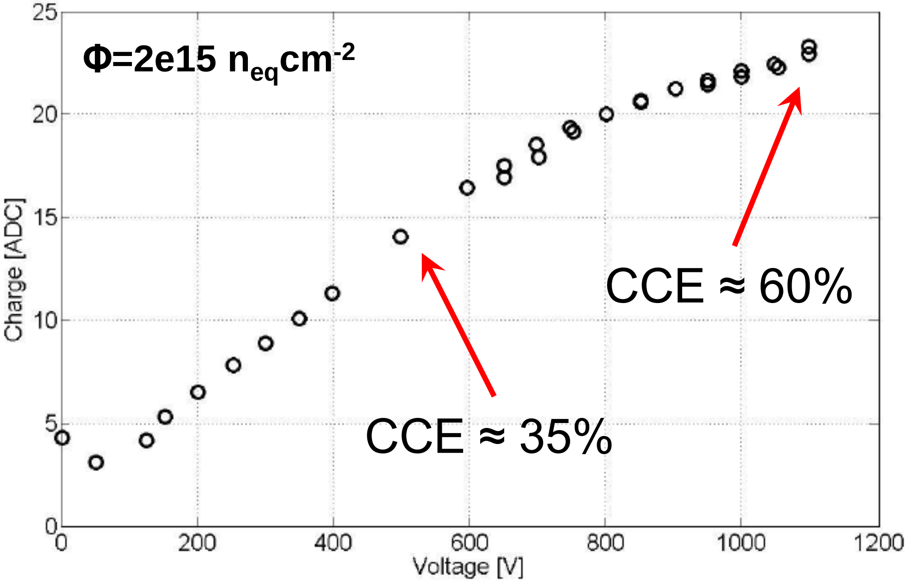

- ☐ **Very high CCE at high V for given fluence & sensor thickness**

Strips @ Φ=2e15 $n_{eq}cm^{-2}$: CCE & CCE(x)

- **Defect model:** proton model at bulk, 3 level model at 2 µm from surface = 'non-unif. 3-level model'
- **Collected charge:** average of CC from MIP injections at midgap & center of strip
- **Q_f = 1.8e12 cm^{-2}:**
  - **p-spray:** strips shorted → defect model not sufficient at high Φ & Q_f
  - **p-stop:** strips isolated
  - **alumina:** Simulation converges only when interface donor traps added (E_V+0.6 eV)

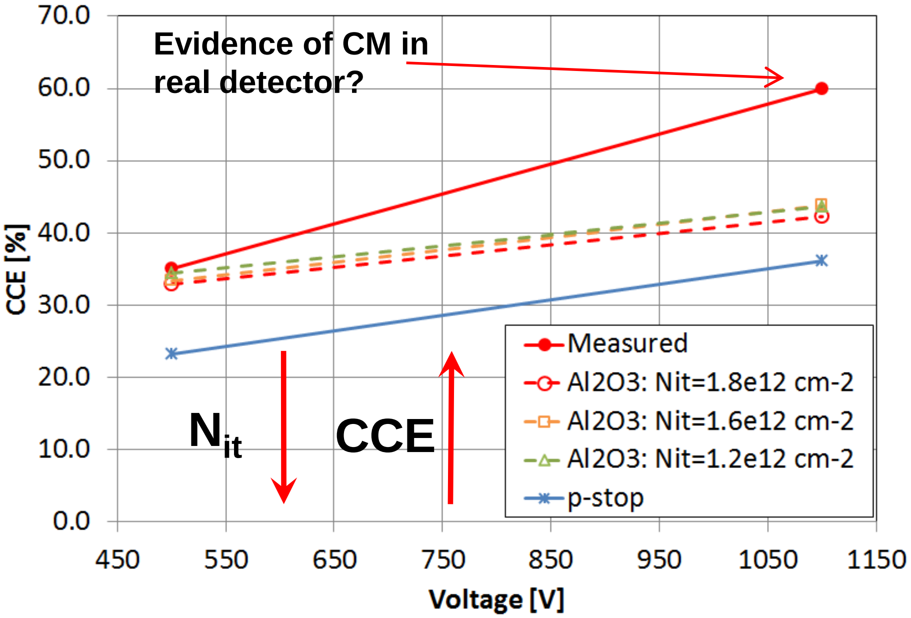

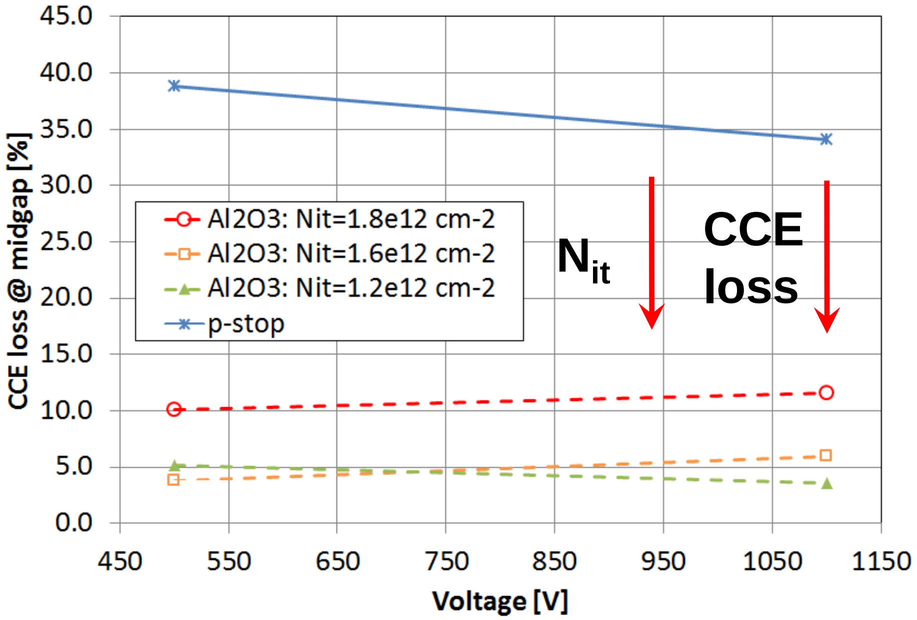

⇨ **Simulations predict very low position dependence of CCE in real sensor with alumina insulator**

Summary

❑ **ALD-grown Al_2O_3 (alumina) field insulator for strip sensors:**

- Low T process < 400° C
- High negative oxide charge after sintering
- Strip sensors show comparable SNR with commercial detectors = good capacitive coupling
- N-on-p detector made by simply one field insulator significantly reduces the complexity & price of sensor processing

Measurement & TCAD simulation study:

❑ **non-irradiated strip sensors:**

- **52 nm alumina:** R_{int} ~500 MΩ → good strip isolation, C_{int} comparable to p-stop values, V_{bd} > 1.5 kV for expected Q_f values

❑ **γ-irradiated MOS structure with 40 nm Al_2O_3:**

- Measurement & simulation results suggest significant accumulation of negative oxide charge

❑ **Proton irradiated strip sensor with 52 nm alumina:**

- High E-fields require implementation of N_{it} to model measured V with realistic Q_f values → with N_{it} very low C_{int}
- High measured CCE at 1.1 kV possibly due to CM → simulations predict very low position dependence of CCE in real sensor

Backup: Publications on ALD

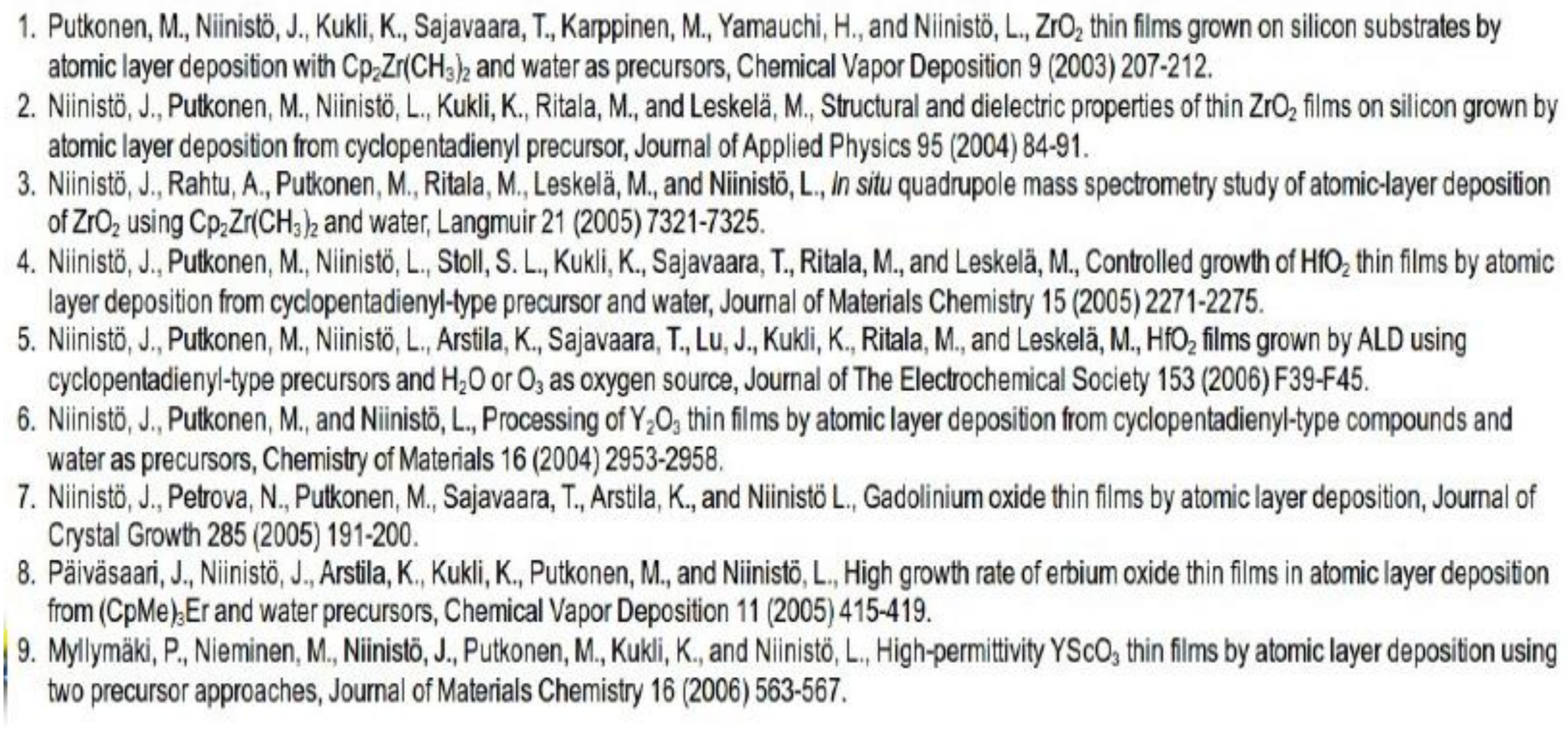

1. Putkonen, M., Niinistö, J., Kukli, K., Sajavaara, T., Karppinen, M., Yamauchi, H., and Niinistö, L., ZrO_2 thin films grown on silicon substrates by atomic layer deposition with $Cp_2Zr(CH_3)_2$ and water as precursors, Chemical Vapor Deposition 9 (2003) 207-212.
2. Niinistö, J., Putkonen, M., Niinistö, L., Kukli, K., Ritala, M., and Leskelä, M., Structural and dielectric properties of thin ZrO_2 films on silicon grown by atomic layer deposition from cyclopentadienyl precursor, Journal of Applied Physics 95 (2004) 84-91.
3. Niinistö, J., Rahtu, A., Putkonen, M., Ritala, M., Leskelä, M., and Niinistö, L., *In situ* quadrupole mass spectrometry study of atomic-layer deposition of ZrO_2 using $Cp_2Zr(CH_3)_2$ and water, Langmuir 21 (2005) 7321-7325.
4. Niinistö, J., Putkonen, M., Niinistö, L., Stoll, S. L., Kukli, K., Sajavaara, T., Ritala, M., and Leskelä, M., Controlled growth of HfO_2 thin films by atomic layer deposition from cyclopentadienyl-type precursor and water, Journal of Materials Chemistry 15 (2005) 2271-2275.
5. Niinistö, J., Putkonen, M., Niinistö, L., Arstila, K., Sajavaara, T., Lu, J., Kukli, K., Ritala, M., and Leskelä, M., HfO_2 films grown by ALD using cyclopentadienyl-type precursors and H_2O or O_3 as oxygen source, Journal of The Electrochemical Society 153 (2006) F39-F45.
6. Niinistö, J., Putkonen, M., and Niinistö, L., Processing of Y_2O_3 thin films by atomic layer deposition from cyclopentadienyl-type compounds and water as precursors, Chemistry of Materials 16 (2004) 2953-2958.
7. Niinistö, J., Petrova, N., Putkonen, M., Sajavaara, T., Arstila, K., and Niinistö L., Gadolinium oxide thin films by atomic layer deposition, Journal of Crystal Growth 285 (2005) 191-200.
8. Päiväsaari, J., Niinistö, J., Arstila, K., Kukli, K., Putkonen, M., and Niinistö, L., High growth rate of erbium oxide thin films in atomic layer deposition from $(CpMe)_3Er$ and water precursors, Chemical Vapor Deposition 11 (2005) 415-419.
9. Myllymäki, P., Nieminen, M., Niinistö, J., Putkonen, M., Kukli, K., and Niinistö, L., High-permittivity $YScO_3$ thin films by atomic layer deposition using two precursor approaches, Journal of Materials Chemistry 16 (2006) 563-567.

Back-up: Measured & simulated CCE(x)

Test beam measurement:

- Strips isolated
- CCE loss between strips ~30%

☐ Traps remove both interface & signal electrons: better radiation induced strip isolation → higher CCE loss between strips

☐ Higher Q_f → more traps filled → charge sharing between strips increases → CCE loss decreases

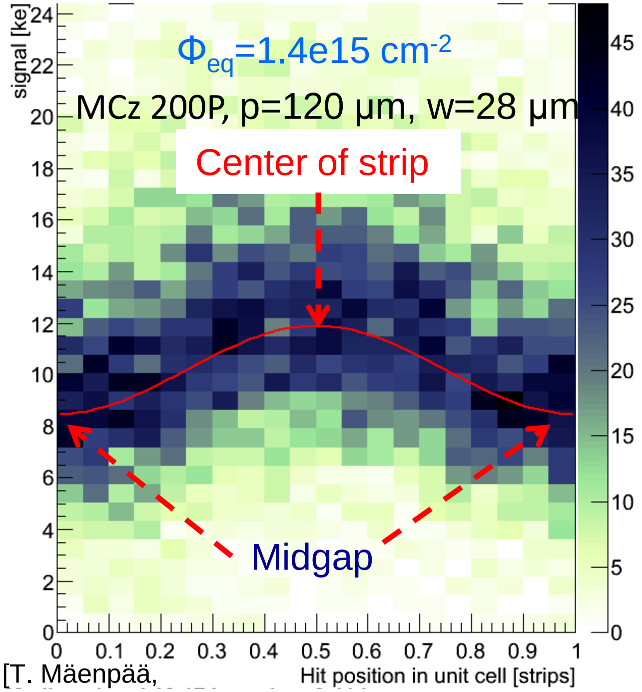
Φ_{eq}=1.4e15 cm^{-2}

MCz 200P, p=120 µm, w=28 µm

Center of strip

Midgap

[T. Mäenpää, PoS(RD13)015, 2013]

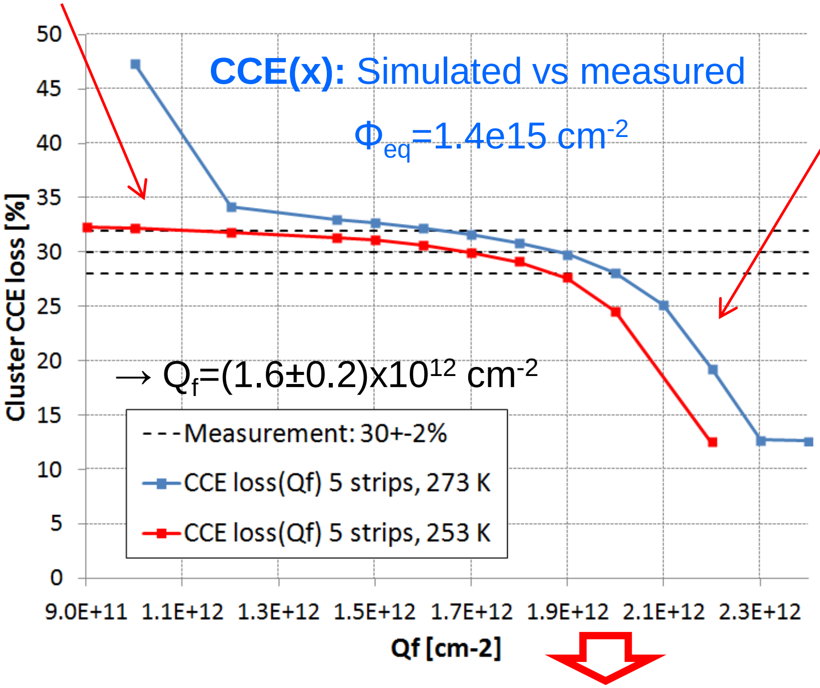
CCE(x): Simulated vs measured

Φ_{eq}=1.4e15 cm^{-2}

→ Q_f=(1.6±0.2)x10^{12} cm^{-2}

☐ **Interpretation:** Irradiation produces non-uniform distribution of shallow traps close to surface → greater drift distance, higher trapping of carriers

[T. Peltola, JINST 9 (2014) C12010]

Preliminary parametrization for **Φ = 3e14 – 1.4e15 cm^{-2}**

Type of defect	**Level** [eV]	**σ_e** [cm^2]	**σ_h** [cm^2]	**Concentration** [cm^{-3}]
Deep acceptor	E_C - 0.525	1e-14	1e-14	1.189*Φ + 6.454e13
Deep donor	E_V + 0.48	1e-14	1e-14	5.598*Φ - 3.959e14
Shallow acceptor	E_C - 0.40	8e-15	2e-14	14.417*Φ + 3.168e16

Backup: SiBT measured CCE loss between strips

Signal loss in-between strips (p=120µm, w/p~0.23)

non-irradiated

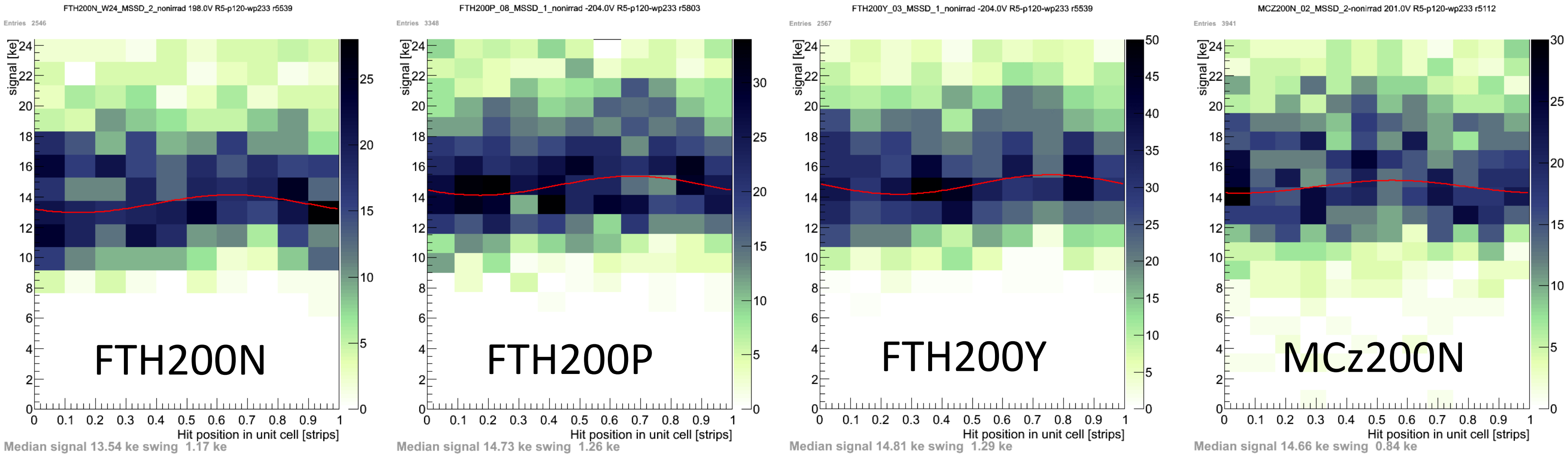

No loss before irrad.; after irrad. ~30% loss; all technologies similar [Phase-2 Outer TK Sensors Review]

mixed irradiated 1.5e15n_{eq}/cm^2